RADIO-SOURCE FRINGE VISIBILITIES WITH AN INTERFEROMETER OF 21500-WAVELENGTH BASE LINE

B. G. Clark and D. E. Hogg
National Radio Astronomy Observatory*
Received November 22, 1965; revised January 14, 1966

ABSTRACT

A survey of 146 radio sources made with the NRAO interferometer at a spacing of 21500 wavelengths and a frequency of 2695 Mc/s has shown that many of these sources have structures of 1″–10″ in size. The results of this survey were compared with those of a similar survey at a lower frequency in an attempt to find a frequency dependence of the source structures. There appears to be no frequency effect for radio galaxies, but quasi-stellar sources have generally higher fringe visibilities at 2695 Mc/s than at 158 Mc/s.

Further investigations were carried out on forty-seven objects showing high fringe visibilities, including the six calibration sources, resulting in the determination of the source brightness distributions for ten small objects and the measurements of positions for thirty-nine objects, six of which are slightly resolved.

I. THE STATISTICS OF FRINGE VISIBILITY

Many observations have been made of fringe visibilities and source brightness distributions with interferometers; however, most of these observations were concerned with sources of special interest rather than with a uniform selection of sources. The statistically most complete survey is that of Allen, Anderson, Conway, Palmer, Reddish, and Rowson (1962) (hereinafter referred to as "AACPRR"), which has been discussed by Allen, Hanbury Brown, and Palmer (1962). These authors demonstrated by statistical arguments that many sources ostensibly larger show fine structure (10″ and smaller) when examined with sufficient resolution. However, since this study was handicapped by uncertainties in the zero-spacing flux of the sources and by low sensitivity, it is worthwhile to check these results and, in addition, to investigate the possible dependence of the brightness distributions on wavelength.

This investigation was conducted with the variable-spacing interferometer of the National Radio Astronomy Observatory. This interferometer consists of two 85-foot paraboloidal antennas operating at a frequency of 2695 Mc/s and, for the present investigation, separated by a distance of 2.4 km, giving a base line of 21574 wavelengths at an azimuth of 242°.

The sample of sources selected for investigation was taken from the list of Pauliny-Toth, Wade, and Heeschen (1966) and consisted of all sources having a peak response in that survey corresponding to a flux density greater than 3.0×10^{-26} W m^{-2} (c/s)$^{-1}$ at 1400 Mc/s. The sources with galactic latitude in the range $\pm 20°$ that were reliably seen as extended by Pauliny-Toth *et al.* (1966), that have a size of 5′ or greater in the 3C or 3C R lists, or that apparently are merely high spots on the galactic ridge were excluded in order to eliminate most of the galactic sources. One source, 3C 61.1, lies beyond the northern declination limits of our telescope and was not observed.

The 146 radio sources so selected were observed near the interferometer equator, so that the effective base line for the observations was uniformly about 21500 wavelengths, although the position angles varied depending on the declination of the source. The interferometer gain was calibrated by assuming that the sources noted as "standard" in the Notes to Table 1 are unresolved at this spacing. The fluxes assumed for these calibrators are also given in Table 1; they were assigned in such a way that, on the mean, these sources lie on the flux scale of Kellermann (1964).

* Operated by Associated Universities, Inc , under contract with the National Science Foundation.

TABLE 1

Fringe Visibilities of Extragalactic Sources Stronger than 3 Flux Units at 1400 Mc/s

Source	Assumed Flux 2695 Mc/s	u	v	γ	No. Obs.	Notes
3C 2	2.1 PTK	19900	8100	0.68	3	(5)
3C 6.1	2.1 PTK	21400	8400	0.54	2	(1)
3C 15	3.0 E	19800	8000	0.14	2	
3C 17	3.9 PTK	19800	8200	0.18	3	
3C 18	2.8 P, PTK	20000	8100	$\leq$ 0.03	3	
3C 19	1.7 PTK	17200	12400	0.14	2	
3C 27	4.0 PTK	19500	7000	0.59	2	
3C 29	3.0 E, K	19900	8000	0.04	2	
3C 31	2.7 e	17400	12100	0.05	2	
3C 32	2.3 E	20000	7900	0.20	2	
3C 33.1	2.0 PTK	19400	6900	$\leq$ 0.05	1	
3C 33	7.2 PTK	19400	9000	0.25	3	
3C 38	2.5 PTK	19400	9100	0.55	2	
3C 40	3.9 E	19900	8100	$\leq$ 0.02	2	
3C 41	2.4 E	19700	8700	0.39	3	
3C 47	2.0 PTK	19300	9400	0.25	2	(5)
3C 48	8.4			1.0		(2) (5)
3C 52	2.1 PTK	15300	15100	0.44	2	
3C 57	2.0 e	20000	7900	0.88	1	
NRAO 91	2.8 PTK	20700	6500	0.99	1	(3)(1)
3C 62	4.0 E	19700	8600	0.10	3	
3C 63	1.9 E	20000	8100	0.07	2	
3C 67	1.6 PTK	18100	11100	0.92	2	
3C 69	2.1 E	13000	20400	0.09	2	(1)
3C 71	3.5 K, E	19300	8100	0.21	1	
3C 75	3.5 P, PTK	20000	8100	0.03	3	
3C 78	5.2 K, P	20000	8100	0.16	2	
3C 79	2.5 P, E, PTK	19700	8900	0.22	2	
3C 84	8.7 B	17400	4100	0.74	2	(4)
3C 86	6.0 E	14200	16200	0.23	2	
3C 88	2.8 P, PTK	11300	9900	0.04	2	(1)
NRAO 140	2.6 PTK	17100	11800	0.98	2	
3C 91	2.0 PTK	18500	10900	0.39	3	
NRAO 150	4.2 PTK	18600	10800	0.80	3	
3C 98	6.6 P, K, E	19900	8400	0.02	3	
3C 105	3.5 P, E	19700	8300	0.40	2	
3C 109	2.5 P, PTK	19500	8800	0.15	2	
3C 111	9.8 E, K	20000	8100	0.04	2	
3C 119	5.1 PTK	19300	9600	0.93	2	(5)
3C 120	3.3 PTK	20000	8200	0.73	3	
3C 123	26.0 PTK, K	19300	9600	0.35	2	
3C 132	2.0 E	19100	9700	0.12	3	
3C 133	3.4 K, E	19600	8900	0.42	2	
3C 134	3.8 PTK	16700	16500	$\leq$ 0.03	2	(1)
3C 136.1	2.3 e	10900	16600	$\leq$ 0.05	2	(1)

TABLE 1 (Continued)

Source	Assumed Flux 2695 Mc/s		u	v	γ	No. Obs.	Notes
3C 138	6.2	K, PTK	19300	9300	0.89	3	(5)
3C 147	11.8				1.0		(2)(5)
3C 153	2.4	E	17400	12700	0.28	2	
3C 154	2.8	PTK	20000	7900	0.21	3	
3C 161	11.4	PK, PTK	19900	8300	0.64	3	
3C 171	2.2	K, PTK	17800	12200	0.18	3	
3C 184.1	4.1	PTK	20300	11200	0.05	2	(1)
3C 192	3.0	E	19900	6700	0.08	3	
3C 195	2.7	E	19600	8700	0.07	3	
3C 196	7.0	K, PTK	16600	13700	0.13	2	(5)
3C 216	2.0	E	13100	16200	0.90	3	(5)
3C 218	21.0	K, PTK	19900	8800	0.11	3	
3C 219	4.5	K, E	18600	10900	0.05	3	
3C 223	1.6	e	19200	9900	≤ 0.04	2	
3C 225	1.8	P	19600	8800	0.65	2	
3C 227	4.2	P, K	19900	7800	≤ 0.05	2	
3C 228	1.8	P	19800	8600	0.19	2	
3C 230	1.5	P	20000	8100	0.96	2	(5)
3C 231	6.4	K	20000	3100	0.09	2	
3C 234	3.5	E, K	20000	7600	0.16	3	
3C 236	2.1	e	19300	9700	0.85	2	
3C 237	3.7	P, K	19900	8700	0.80	3	
3C 244.1	1.8	e	15600	14900	0.50	3	
3C 245	2.0	P	19900	1600	0.60	3	(5)
3C 254	1.8	E	18400	11200	0.61	3	(5)
3C 263	1.6	PTK	20000	2300	0.64	2	(5)
3C 263.1	1.4	e	20000	9600	0.12	3	
3C 264	3.5	PTK	19900	8000	0.08	2	
3C 268.1	4.5	e	20000	3100	0.63	3	
3C 268.3	2.2	e	12900	17200	0.79	3	
3C 270	12.4	PK	19900	7900	0.02	3	
3C 272.1	4.4	E	19900	8300	0.03	3	
3C 273	37.3	PK	20000	8100	0.91	2	(5)
3C 274	123.	BMW	19900	8400	0.03	2	
3C 274.1	1.5	e	19800	8500	0.11	3	
3C 275	1.2	E	20000	8100	0.52	3	
3C 277.3	2.0	e	19800	8500	0.06	3	
3C 278	4.6	K, E	19800	8500	≤ 0.03	2	
3C 279	12.5	PK	20000	8000	0.86	3	(5)
3C 280	3.4	E	17000	13300	0.88	1	
3C 287	4.4	K	19000	10000	1.03	3	(5)
3C 286	10.7				1.0		(2)(5)
3C 288	1.8	e	19600	8800	0.20	4	

TABLE 1 (Continued)

Source	Assumed Flux 2695 Mc/s		u	v	γ	No. Obs.	Notes
3C 293	3.1	PTK	19000	10200	0.65	2	
3C 295	11.7	K, PTK	19500	8500	0.87	3	
3C 296	3.2	e	20000	7800	0.03	2	
3C 298	2.7	P	19900	7900	0.88	3	(5)
3C 300	1.7	e	19200	9500	0.25	3	
3C 305	2.2	PTK	13100	17100	0.32	3	
3C 309.1	5.1	PTK, K	19900	4700	0.93	3	(5)
3C 310	3.3	K, E	19700	8900	0.02	2	
3C 313	1.7	P	19900	7700	0.34	2	
3C 315	2.6	E	19600	9100	$\leqslant$ 0.03	1	
3C 317	2.0	P, E	19800	8400	0.16	3	
3C 321	1.8	e	19800	8600	0.20	3	
3C 325	2.1	e	7000	20400	0.51	2	
3C 327	4.4	PK, PTK	19900	8100	0.08	3	
3C 327.1	2.1	P	19900	8200	0.43	3	
3C 330	4.4	E	5000	21000	0.46	2	
3C 338	1.8	K, E	19900	7200	0.06	3	
3C 337	1.8	e	19700	8000	0.31	2	
3C 343	2.4	M	16100	9000	0.98	2	(4)
3C 343.1	2.2	M	9400	19400	1.01	4	
3C 345	5.8				1.0		(2)(5)
3C 346	2.2	e	20000	7800	0.20	3	
3C 348	24.0	K, PTK	19900	8200	0.01	3	
3C 349	1.9	e	17900	12000	0.37	3	
3C 351	1.8	e	12900	17300	0.42	3	(5)
3C 353	31.0	K, PTK	19900	8100	$\leqslant$ 0.01	1	
NRAO 530	4.3	PTK	19200	9200	0.86	2	
3C 380	8.8				1.0		(2)(5)
3C 381	2.7	e	14100	15900	0.19	2	
3C 382	3.5	e	19100	10100	0.06	2	
3C 386	4.0	P, K	19900	8400	$\leqslant$ 0.02	3	
3C 388	3.6	K	17300	12900	0.06	3	
3C 390	2.9	E	19900	8300	0.39	2	
3C 390.3	6.4	PTK	16200	17000	0.57	1	(1)
3C 395	1.7	e	19300	9600	1.32	2	
3C 396	10.0	PTK	19900	9200	$\leqslant$ 0.01	3	
3C 401	3.5	E	15200	15300	$\leqslant$ 0.02	4	
3C 403	3.7	P, K	19800	8200	0.04	4	
3C 405	783.	BMW	18800	10600	0.07	2	
3C 409	5.5	K, PTK	18100	10800	0.05	2	
3C 410	6.0	K, PTK	18700	10600	0.70	4	
3C 411	1.4	P	19200	8900	0.42	4	
3C 418	3.9	K	15000	15400	1.02	1	
3C 427.1	2.0	E	21700	7800	0.47	1	(1)

TABLE 1 (Continued)

Source	Assumed Flux 2695 Mc/s	u	v	γ	No. Obs.	Notes
3C 430	4.6 K, E	15100	15400	0.08	2	
3C 431	1.5 E	16200	14200	0.35	2	
3C 433	6.3 K	19900	8100	0.08	3	
3C 436	2.1 E	19900	8000	$\leqslant$ 0.07	3	
3C 438	3.4 K	19800	8000	0.50	3	
3C 440	1.9 e	13700	16600	0.67	3	
3C 444	4.6 PK	15200	11600	$\leqslant$ 0.02	2	
3C 445	3.7 E	19900	8200	$\leqslant$ 0.04	4	
3C 446	4.4 PTK, E	19900	7900	0.83	2	(5)
3C 452	6.4 K, E	18200	11600	0.02	3	
3C 454.3	9.7 PK, K	19800	8500	0.91	3	(5)
3C 459	2.3 P, PTK	20000	8000	0.58	2	
3C 465	3.3 K	19100	9800	0.09	3	
3C 468.1	1.8 PTK	10400	18900	0.91	3	

Flux References:

K Kellermann (1964)
BMW Baars, Mezger, and Wendker (1965a)
B Baars, Mezger, and Wendker (1965b)
P Day, Shimmons, Eckers, and Cole (1965)
M Moffet (1965)
PK Kellermann (Parkes measurements, unpublished)
PTK Pauliny-Toth and Kellermann (unpublished measurements)
E Extrapolated from measurements at lower frequencies
e Extrapolated from Pauliny-Toth *et al.* (1966) measurements at 1400 and 750 Mc/s only.

Table 1 Notes

(1) Measurement made at 2700 m antenna spacing during another series of measurements.

(2) Angular size and flux standard - Assumed unresolved.

(3) NRAO 91 incompletely observed by Pauliny-Toth *et al.* is Parkes source 0202 + 14

(4) Measurement made at 2100 m antenna spacing during another series of measurements.

(5) Identified as a quasistellar source. Most are from the summary of Wyndham (1966).

In order to derive fringe visibilities, a zero-spacing flux must be assumed. Because only long base lines are accessible to this instrument, the fluxes must be taken from the work of other observers. The origins of the fluxes used are given in Table 1, along with their values. The uncertainty introduced into the visibilities by the uncertainty of the assumed fluxes appears to average about 15 per cent, though in many cases it is lower when, e.g., a strong source has been carefully observed at 2695 Mc/s. In some cases, where the flux has been extrapolated from lower frequencies, the uncertainty is higher since the source spectrum may be curved.

The observed fringe visibilities are given in Table 1. In the first two columns are the source name, flux density, and the reference for the measurement of flux density. Those

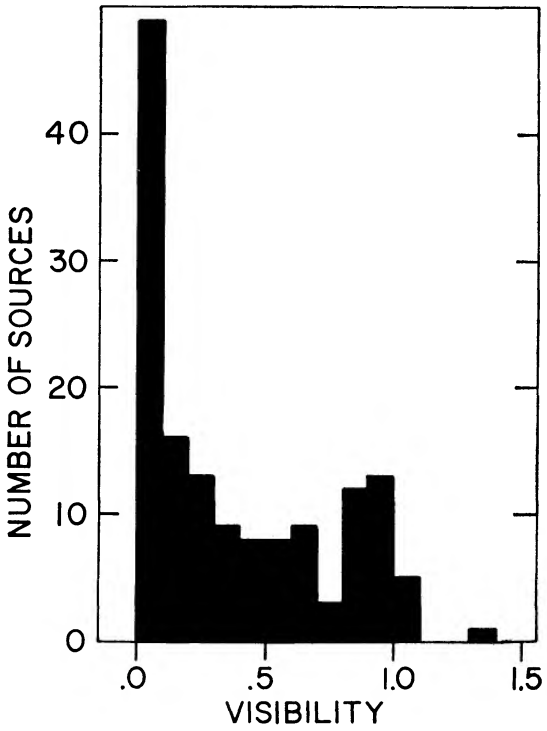

FIG. 1.—Histogram of fringe visibilities for the sample of sources observed with a 21500-λ base line

sources listed as NRAO followed by a number are sources appearing in the catalogue of Pauliny-Toth *et al.* (1966) but not in 3C or 3C R. The next two columns describe the resolving power of the interferometer for this observation, u being the right-ascension component of the effective base line and v the declination component. In the last column is given the fringe visibility, γ. The error in the fringe visibility is about 15 per cent from the error in the assumed zero-spacing flux or the error resulting from an uncertainty of 0.1 flux unit in the flux measured with the interferometer, whichever is greater.

A histogram of the distribution of fringe visibilities is given in Figure 1. This distribution of visibilities appears to be independent of galactic latitude which confirms that most of the sources of this survey are extragalactic. Under certain assumptions the distribution of visibilities may be converted into the distribution of angular sizes. Thus, e.g., if it is assumed that all sources are simple circular Gaussians, then the histogram of Figure 1 implies a roughly uniform distribution of the sizes of the Gaussians out to about 11″ half-width, after which there is a much reduced incidence. Only 49 of the 146 sources in this sample have visibilities less than 0.1, corresponding to a Gaussian of 8″ half-width or greater.

The assumption of Gaussian brightness distributions is, of course, unrealistic, as many radio sources are actually double with a fairly large ratio of separation to component size. In this case, however, the above argument applies with very little modification to component sizes. The only effect of the double nature of the sources is to smear the histogram and shift it toward zero visibility. We may thus conclude that the component sizes are, for the most part, less than 10″. It is also of interest to compare Figure 1 with the histograms given by Allen, Hanbury Brown, and Palmer (1962). Although at first sight these are quite different, the difference lies principally in the lower range of visibility where AACPRR have only upper limits on the visibilities of many sources. In the present investigation we detected all but sixteen of the sources, and the upper limits set for the

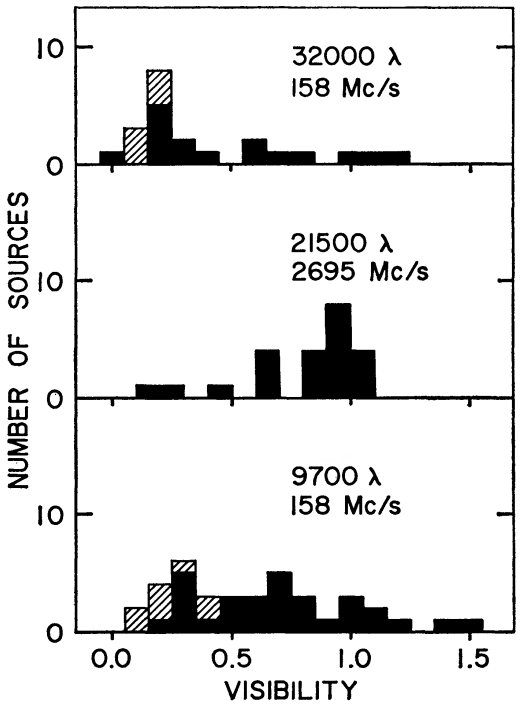

FIG 2 —Comparison of the visibilities of quasi-stellar sources at two frequencies *Top* and *bottom*, prepared from the data of Allen, Anderson, Conway, Palmer, Reddish, and Rowson (1962) (158 mc/s); *center*, the present survey.

visibilities of these sixteen were all less than 0.1, so that even these may be assigned to a unique column in the histogram. When this is taken into account there may be only small differences between the histograms of Allen, Hanbury Brown, and Palmer and Figure 1. For instance, although the percentage of sources in this investigation with visibilities greater than 0.5 (37 per cent) is slightly greater than that expected by interpolation between the 9700- and 32000-wavelength values of Allen, Brown, and Palmer (23 per cent), there is a 10 per cent probability that a difference this great or greater could result from chance alone.

Although the results of this survey and that of AACPRR are similar if all sources are included, there is a significant difference between the two surveys if only those radio sources identified with quasi-stellar objects are considered. The histogram found for the quasi-stellar sources in our sample is given in Figure 2, along with the histograms prepared from the data of AACPRR. Filled blocks in the histogram indicate the exact measurement. Shaded blocks are upper limits only and are assigned to the first column lower than the limit. Whereas in the present data the median fringe visibility is 0.9, that

of AACPRR at 9700-λ base line is 0.6, with 43 per cent having visibilities less than 0.5. Therefore, it appears that the structure of quasi-stellar sources is dependent on frequency. The observations would be satisfied if the quasi-stellars have large-scale structure with a steeper spectrum than the "core"; the large-scale structure would dominate at 158 Mc/s but would not contribute a significant part of the flux at 2695 Mc/s. This sort of behavior is known to occur in at least one source, 3C 273. This source is large (20″) and double at low frequencies, but at higher frequencies (Adgie, Gent, Slee, Frost, Palmer, and Rowson 1965) most of the flux comes from a quite small region (0.″4).

Although it is rather difficult to compare the present data with those of AACPRR on a source-by-source basis because of the sparsity of points where the visibilities have been measured and because of the large errors quoted by AACPRR, there are three sources which clearly show a frequency-size dependence. Possibly the most interesting case is 3C 279, for which Palmer (1965) gives a diameter of 25″, whereas it is unresolved, with an upper limit of 3″ in position angle 60°, in this investigation. The spectrum of 3C 279 is known to have a distinct minimum near 1400 Mc/s. It would be natural to assume that the decreasing component of the spectrum is of large angular size and the increasing component is of extremely small size; however, if the spectra of the two components are linearly extrapolated, the decreasing component contributes 35 per cent of the flux at 2695 Mc/s. We do not observe a large halo of this flux density. Since our visibility is 0.8 or greater, any extended component must contribute less than 20 per cent of the total flux. High-resolution observations near the minimum in the spectrum would further illuminate this problem.

The second source for which the present observations disagree with those of Palmer (1965) is 3C 245. Palmer suggests that the size is 10″; the present observations agree with the decimeter-occultation result of Hazard, Mackey, and Nicholson (1964) in describing the brightness distribution as a double source with small components and a separation of approximately 3″. Finally, the size quoted by Palmer (1965) for 3C 241 is 23″, as compared with an upper limit of 3″ in position angle 65° determined by our observations (see § II below).

The differences between Figure 1 and the histograms of Allen, Hanbury Brown, and Palmer (1962) although not in themselves statistically significant, are about those to be expected from the number of quasi-stellar sources in the sample, given the behavior of Figure 2. It thus seems likely that for radio galaxies the histogram of Figure 1 is not very different from the histograms at 158 Mc/s, suggesting that there is no apparent systematic difference in the brightness distributions at the two frequencies. This conclusion refers primarily to the structure in the size range 3″–10″, as differences in large structure may be concealed by the generally low fringe visibilities and smaller structure is unresolved. It is still possible that radio galaxies also have a low-frequency halo of size larger than 10″, unnoticed here because of the small number of radio galaxies with high fringe visibilities, where the effect would be most apparent. It would be most desirable to obtain detailed brightness distributions for both the quasi-stellar sources and the radio galaxies at both frequencies; however a statistical investigation of the occurrence of halos in radio galaxies would be of interest and can best be made using interferometers with shorter base lines.

II. THE SOURCES OF SMALL ANGULAR DIAMETERS

In addition to the survey of the brightest sources we also observed near the interferometer equator a number of sources of special interest. First, we examined several galactic sources, both thermal and non-thermal, in an attempt to find "hot spots" in sources already resolved with much shorter spacings. These sources show uniformly low visibilities, which eliminates the possibility that the sources are composed of a very few hot spots with brightness temperatures of tens of thousands of degrees.

Next, we examined a group of sources known or suspected to be small: sources showing a high visibility in the survey of AACPRR; sources showing interplanetary scintillation

(Hewish, Scott, and Wills 1964); and sources suggested to be quasi-stellars. The results are shown in Table 2.

From Tables 1 and 2 we selected for further study thirty-nine sources having high fringe visibility. These were observed at various hour angles across the sky, varying the length and position angle of the effective base line. The right-ascension component u and the declination component v of the effective base line are given by (see, e.g., Rowson 1963):

$$u = B_2 \sin (H - h) , \qquad v = B_1 \cos \delta - B_2 \sin \delta \cos (H - h) , \tag{1}$$

where the base-line constants for this base line are

$$B_1 = \frac{D}{\lambda} \sin d = 7104.2 , \qquad B_2 = \frac{D}{\lambda} \cos d = 19993.0 , \qquad h = -7^{h}10^{m}27^{s}.4 , \tag{2}$$

and H is the hour angle of the observation.

Twenty-nine of these thirty-nine sources are indeed unresolved with a 21500-λ base line. The size limits for these sources are given in Table 3. The fringe visibilities of the remaining ten as a function of hour angle are shown in Figures 3 and 4. From this rather limited sampling of points in the uv-plane we cannot uniquely reconstruct the true brightness distribution, so we have tried to fit the observations with one of several models. We

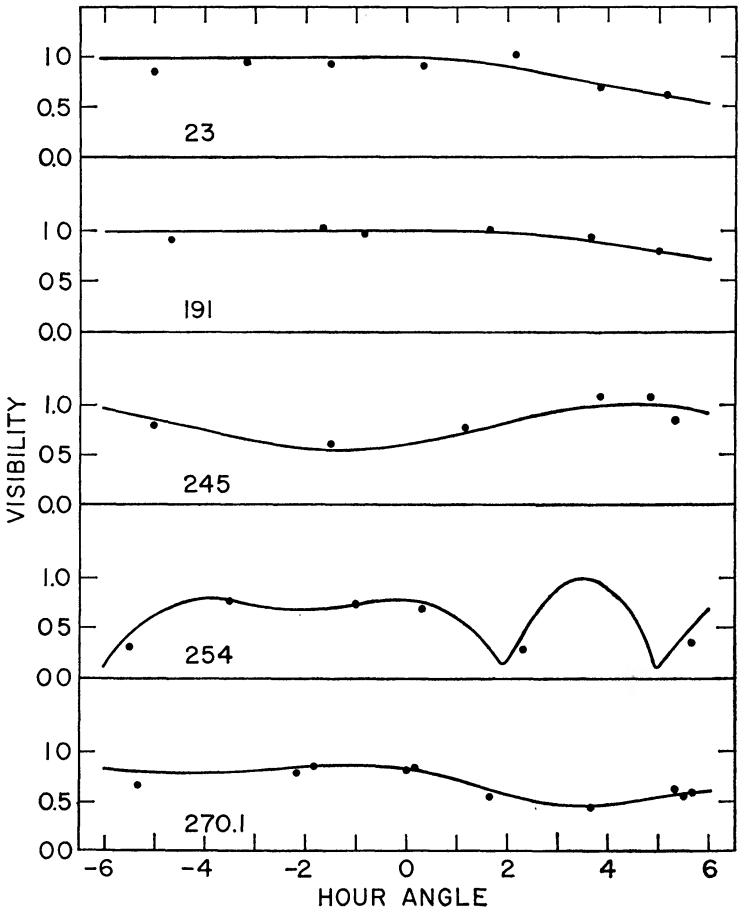

FIG. 3.—Radio-source fringe visibilities as a function of hour angle. *Solid curve:* proposed source model.

TABLE 2
Fringe Visibilities of Various Weak and Galactic Sources

Source	Assumed Flux 2695 Mc/s		u	v	γ	No. Obs.	Notes
MSH 00-29	1.6	P	19300	4400	0.21	2	(1)
3C 10	28.0	K	11500	18300	$\leq$ 0.003	3	(2)
3C 23	0.7	P	18400	10100	0.83	1	
3C 54	1.2	E	18500	11100	0.15	3	
3C 58	33.7	H	6800	20500	$\leq$ 0.002	3	(2)
3C 61	0.5	E	19800	8500	0.68	2	
3C 83.1	5.0	K, E	16100	14000	$\leq$ 0.02	3	
3C 85	0.8	E	18700	9900	0.25	3	
3C 93	1.5	PTK	19700	8400	0.30	2	(1)
MSH 03-19	3.5	P, E	19900	8400	$\leq$ 0.03	2	
3C 107	0.8	PTK	19500	8000	0.45	3	
3C 144	748.	H	19000	9800	0.0006	2	(2)
3C 145	411.	H	20000	8200	$\leq$ 0.0005	1	(3)
3C 147.1	60.	BN	20000	8100	$\leq$ 0.002	2	(3)
3C 152	0.6	e	19300	9500	1.10	3	(4)
3C 158	1.2	PTK	19600	8800	0.62	2	(4)
3C 186	0.6	E, PTK	19600	8700	0.94	1	(4) (1)
3C 191	0.8	P	19900	8300	0.96	2	(4) (1)
3C 208	1.2	P	20000	7700	0.60	1	(1)
3C 208.1	1.2	PTK	19800	8600	0.60	2	
3C 222	0.4	e	19800	7900	0.89	3	
3C 238	1.2	P, PTK	19900	7800	0.89	2	(4)
3C 241	0.8	e	19600	8900	0.89	2	(4)
3C 255	0.7	e	20000	8100	0.91	2	(4)
3C 256	0.7	e	19900	8300	0.92	2	
3C 270.1	1.5	PTK	18600	10800	0.82	2	(1)
W 22	30.	BN	19500	4200	$\leq$ 0.003	3	(3)
3C 358	10.2	H	18300	4600	$\leq$ 0.01	3	(2)
SGR A	65.	H	19300	4500	0.005	3	
W 28	25.	BN	18600	4500	$\leq$ 0.003	3	(2)
W 29	12.	BN	19300	4400	$\leq$ 0.014	3	(3)
W 31	5.8	BN	18300	4900	$\leq$ 0.02	3	(3)
W 37	19.	H	19700	8600	$\leq$ 0.004	3	(3)
W 38	55.	BN	19600	8800	$\leq$ 0.002	2	(3)
W 52	8.5	K	19600	8900	0.02	4	(3)
3C 392	130.	E	19600	8800	$\leq$ 0.005	4	(2)
3C 400	500.	e	19900	8600	$\leq$ 0.0005	3	(3)
MSH 19-111	3.7	E	19900	7300	0.62	4	
3C 422	1.3	E	19900	8000	0.90	3	
NRAO 684	1.3	e	16900	13000	0.28	3	
NRAO 686	0.7	e	18800	10600	0.22	3	
NRAO 689	0.4	e	18200	11500	$\leq$ 0.20	3	
NRAO 690	0.7	e	16600	13300	$\leq$ 0.10	3	
3C 455	1.4	PTK	19800	8500	0.47	3	(1)
MSH 23-112	1.0	E	19900	8300	0.48	3	
CTA 102	4.5				1.0		(5) (1)

Flux References: Same as Table 1 with, in addition, H, from spectrum in Howard and Maran (1964) catalogue, and BN, Altenhoff et al. (1961)

Table 2 Notes

(1) Suggested quasi-stellar sources
(2) Non-thermal galactic source
(3) Thermal galactic source
(4) Hewish scintillator
(5) Angular size and flux standard; assumed unresolved.

TABLE 3

Unresolved Sources

Source	Size Limits
3C 2	< 2".5 in P. A. 90° May be extended ~ 6" in P. A. 0° or may have large halo ~ 25% of the flux
3C 57	< 3" in P. A. 65°
3C 67	< 3".5 in any direction
NRAO 150	< 3" in any direction
3C 119	< 3" in any direction
3C 138	< 2".5 in P. A. 60° < 3".5 in any direction
3C 152	< 2".5 in P. A. 70° < 4" in any direction
3C 186	< 4" in any direction
3C 216	< 2".5 in any direction
3C 222	< 2".5 in P. A. 60° < 7" in any direction
3C 230	< 2".5 in P. A. 65°
3C 236	< 3" in any direction
3C 237	< 2".5 in P. A. 65° < 8" in any direction
3C 238	< 3" in P. A. 65° < 8" in any direction
3C 241	< 3" in P. A. 65° < 6" in any direction
3C 255	< 3" in P. A. 60°
3C 256	< 3" in P. A. 60°
3C 268.3	< 3" may have ~ 15% of flux in large halo or assumed flux may be in error.
3C 279	< 3" in P. A. 60° < 20% large halo
3C 287	< 2".5 in P. A. 60° < 4" in any direction
3C 293	< 3" in P. A. 65° < 5" in any direction Perhaps 25% large halo, or this may be an error in assumed flux.
3C 298	< 2".5 in P. A. 65°
3C 309.1	< 2".5 in any direction
3C 318	< 3" in P. A. 40° < 5" in any direction
NRAO 530	< 3" in P. A. 65°
3C 418	< 3" in any direction. There may be 25% large halo.
3C 422	< 2".5 in P. A. 70°
3C 446	< 3" in P. A. 65°
3C 454.3	< 2".5 in P. A. 70° < 5" in any direction

have used, in order of complexity, the following models: (1) circular Gaussian, (2) point double with equal components, (3) equal double with circular Gaussian components, (4) unequal double with circular Gaussian components.

For each source we give below the simplest of these possibilities that fits the observed data. The visibilities resulting from these models are shown as lines in Figures 3 and 4. The observations are not sufficiently continuous that we may sort out the effects of a

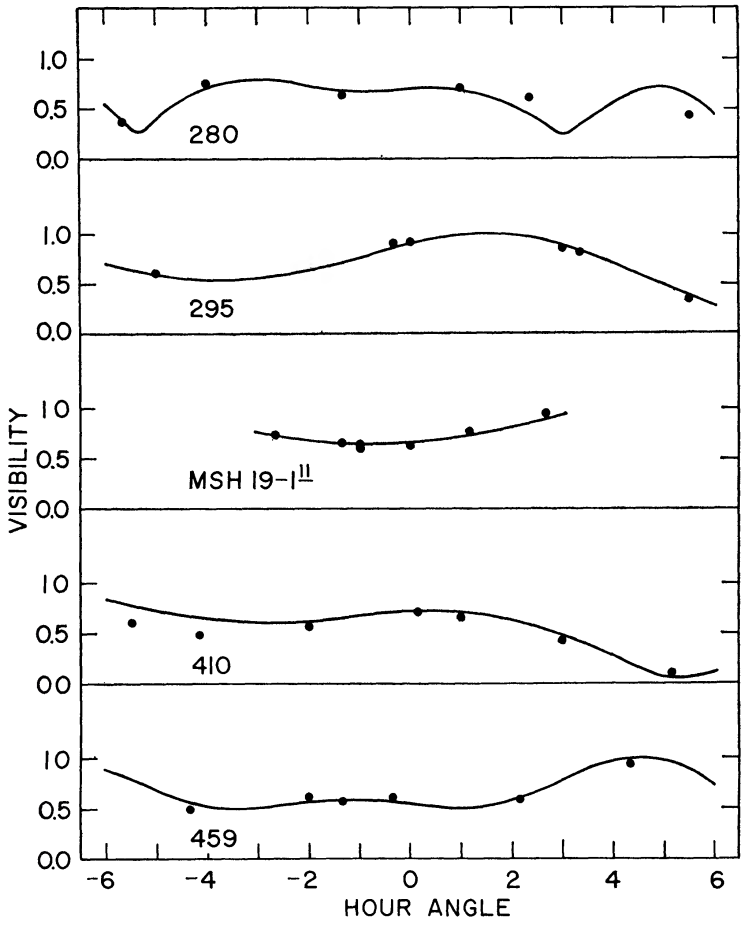

FIG. 4.—Radio-source fringe visibilities as a function of hour angle. *Solid curve:* proposed source model.

varying visibility phase from those of an error in the assumed source position, so for those sources that we find to be unequal doubles, we are unable to say which is the stronger component.

We have determined the brightness distributions of the following resolved sources:

3C 23.—Point double 4".5 separation in position angle 160° ± 20°.

3C 191.—The observations at large hour angle may be erroneous for this source. It may be completely unresolved. Plotted in Figure 3 is the visibility-curve of a point double separated 4".0 in P.A. 155°. The width of the source in P.A. 65° is less than 2".5.

3C 245.—Possibly a point double of 3".5 separation in P.A. 100°. Because of the nearness of this source to the equator, the range in v is not well covered, so that the position angle is poorly determined.

3C 254.—Double source extended 13".5 in P.A. 110°. The components appear to be

TABLE 4

Source Position Measurements

o. bs.	Source	R.A. (1950.0)	Dec. (1950.0)	R.A. Difference (Radio–Optical)	Dec. Difference (Radio–Optical)	N O
3	3C 2	$00^h03^m48^s.76\pm.11$	(−00°21'21")	$+0^s.06\pm0^s.11$	(−14")	
2	3C 23	00 49 08.77±.09	+17°30'58".9±3.5			
5	3C 48	01 34 49.82±.06	+32 54 21.1±1.6	+ .00± .06	+0".9± 1".6	2
1	3C 57	01 59 30.44±.30	−11 47 12.3±15.			
3	3C 67	02 21 18.04±.08	+27 36 39.3±2.0			
3	3C 84*	03 16 29.58±.08	+41 19 52.3±1.7	+ .18± .08	+0.3± 1.7	
4	3C 119	04 29 07.94±.13	+41 32 09.6±1.9	+ .10± .13	+0.9± 1.9	
2	3C 138	05 18 16.65±.10	+16 35 28.5±3.5	+ .14± .10	+2.3± 3.5	
3	3C 147	05 38 43.52±.11	+49 49 42.9±1.8	− 01± .11	−0.2± 1.8	1
4	3C 152	06 01 30.30±.14	+20 21 35.9±2.7			
3	3C 186	07 40 56.81±.09	+38 00 31.6±1.5	+ .14± .09	−0.3± 1.5	
3	3C 191	08 02 03.72±.52	+10 24 36.1±24.	− .06± .52	38.0±24.	
2	3C 216	09 06 17.30±.11	+43 05 56.0±1.7	+ .04± .11	−3 0± 1.7	
3	3C 236	10 03 05.40±.08	+35 08 43.3±1.8	+ .01± 08	+5.2± 1.8	
2	3C 237	10 05 22.02±.10	+07 44 53.8±10.	− .05± .10	−6.0±10.	
3	3C 238	10 08 23.02±.10	+06 39 18.2±12.			
3	3C 241	10 19 09.38±.09	+22 14 38.5±2.9			
2	3C 245	10 40 06.00±.10	+12 19 17.1±5.	− .11± .10	+2.0±5.	
2	3C 255	11 16 52.14±.12	(−02 46 40)			
1	3C 256‡	11 18 04.71±.13	+23 45 08.5±4.5	2.52± .13	52.7±4.5	
4	3C 268.3	12 03 54.36±.27	+64 30 15.2±2.4			
2	3C 273†	12 26 33.27±.11	(02 19 38)	− .04± .11	(−6)	
3	3C 279	12 53 35.87±.14	−05 31 23.8±22.	− 07± .14	−15.8±22.	
4	3C 287	13 28 15.96±.08	+25 24 38.4±2.2	− .16± .08	1.3±2.2	
1	3C 286	13 28 49.66±.06	+30 45 59.0±1.7	− .08± .06	−0.5±1.7	2
2	3C 293	13 50 03.20±.14	+31 41 30.0±3.5	− .22± .14	−2.2±3.5	
4	3C 295	14 09 33.50±.12	+52 26 13.6±1.8	+ .06± .12	+0.0±1.8	
2	3C 298	14 16 38.68±.15	+06 42 21.6±14.	− .14± .15	0.0±14.	
3	3C 309.1	14 58 59.27±.17	+71 52 12.6±2.3			
3	3C 318	15 17 50.96±.26	+20 26 51.6±9.3	.22± .26	−1.9±9.3	
0	3C 345	16 41 17.62±.07	+39 54 11.5±1.6	− .08± .07	+0.4±1.6	1
2	AO 530	17 30 13.62±.15	−13 02 49.1±8.			
.2	3C 380	18 28 13.41±.10	+48 42 39.9±1.8	+ .03± .10	+0.6±1.8	1
2	SH 19-111	19 38 24.32±.18	−15 31 34.0±7.8			
6	3C 418	20 37 07.24±.12	+51 08 36.6±1.8			
1	3C 422	20 44 34.21±.24	(02 47 56)			
2	3C 446	22 23 10.96±.13	−05 12 08.8±25.	.09±.13	8.2±25.	
2	TA 102	22 30 07.76±.09	+11 28 19.5±5.5	.05±.09	3.3±5.5	
3	3C 454.3	22 51 29.54±.16	15 52 54.2±12.			

Parenthesized positions from Pauliny-Toth et al.

* May be affected by large diameter halo.

† Refers primarily to component B, may be affected by presence of component A.

‡ Note added in proof: Our observations of 3C 256 are also consistent with a position of $\alpha = 11^h\ 18^m\ 04^s.18 \pm.15$, $\delta = 23°\ 44'\ 19".8 \pm5.0$. We are indebted to R. L. Adgie for pointing out that this position is probably the correct one.

extended with sizes about 3″.5. Observations made in another investigation at the minimum at H.A. $+2^h$ showed that the minimum visibility was about 0.1, suggesting a component ratio of 1.2:1.0. This determination depends on the assumption that the components have the same size.

3C 270.1.—Double separated 7″.5 in position angle 160°, component ratio 3:1. The components may be slightly extended, ~2″.

3C 280.—Apparently double with separation 11″.5 in P.A. 90° ± 7° and component ratio 2:1 with 3″ component sizes. The component size is rather uncertain because of the uncertainty of the flux.

3C 295.—The observations are fitted sufficiently well by an equal point double with 4″.5 separation in P.A. 135° ± 15°. This is in satisfactory agreement with the observations of Anderson, Palmer, and Rowson (1962), who find a separation of 4″ in P.A. 135° with components 1″.7 × <1″.

MSH 19-111.—Point double of separation 3″.5 in P.A. 110° ± 25°. The position angle is very poorly determined because the resolving power of the interferometer for this source is never very great except in position angles near 70°.

3C 410.—Equal double separation 6″.5 in P.A. 150° ± 10°, 3″ components.

3C 459.—Unequal point double 6″.5 separation in P.A. 95° ± 20°, with component ratio 3:1. The size of the components does not exceed 3″.5.

The observations made here were sufficient for the determination of the positions of the unresolved sources. The method outlined by Wade, Clark, and Hogg (1965) was used. The base-line constants used here were chosen to make the radio positions agree in the mean (weighted, of course, according to the error of each determination) with the optical positions for all of the identified sources, rather than basing the calibration on only a few well-known identified sources as did Wade *et al.* (1965). The results of these position determinations are given in Table 4. This table contains determinations for some of the small resolved sources as well as the unresolved sources of Table 3 and the standard calibrator sources. Also included are results on 3C 84 and 3C 273, which were observed in another program. We feel that the measurements for these slightly resolved sources are not too strongly influenced by a changing visibility phase, so that the position derived by this method is not far from the center of gravity of the source. Table 4 also includes the displacement from the optical position for those identified sources that have an accurately measured optical position. The small size of these displacements, in most cases, confirms the identifications.

This investigation, coupled with previous ones, especially AACPRR, not only has indicated that many radio sources have interesting structure in the size scale from 1″ to 10″ but has provided a finding list of sources which may be used to calibrate the gain and phase of an instrument of 10″ resolution. Investigation of these sources by an instrument of 1″ resolving power is desirable in order to determine their brightness distribution.

We wish to thank I. Pauliny-Toth and especially K. Kellermann for assistance with the zero-spacing fluxes. They have made available to us unpublished observations and have been very helpful in several discussions. We also wish to thank P. Véron for a list of accurate optical positions made available to us before publication. These observations would have been impossible without the work of W. Tyler on the receivers and systems.

REFERENCES

Adgie, R. L., Gent, H., Slee, O. B., Frost, A D , Palmer, H. P., and Rowson, B. 1965, *Nature*, **208**, 275.
Allen, L. R., Anderson, B., Conway, R. G., Palmer, H. P., Reddish, V. C., and Rowson, B. 1962, *M.N.*, **124**, 477 ("AACPRR").
Allen, L. R., Brown, R Hanbury, and Palmer, H. P. 1962, *M.N.*, **125**, 57.

Altenhoff, W , Mezger, P. G., Wendker, H., and Westerhout, G. 1960, *Veröff Univ. Sternwarte Bonn*, No. 59, Part IV.
Anderson, B., Palmer, H. P., and Rowson, B. 1962, *Nature*, **195**, 165.
Baars, J. W. M., Mezger, P. G., and Wendker, H. 1965*a*, *Ap. J.*, **142**, 122
———. 1965*b*, *Nature*, **205**, 488.
Day, G , Shimmons, A. J., Eckers, R., and Cole, D. 1966, *Australian J. Phys.*, **19**, 35.
Hazard, C., Mackey, M. B , and Nicholson, W. 1964, *Nature*, **202**, 227.
Hewish, A., Scott, P. F., and Wills, D. 1964, *Nature*, **203**, 1214.
Howard, W. E , and Maran, S. P. 1965, *Ap. J. Suppl* , **10**, 1.
Kellermann, K I. 1964, *A.J* , **69**, 205.
Moffet, A. T. 1965, *Ap. J* , **141**, 1580.
Palmer, H P 1965, paper presented at 2d Texas Symposium on Relativistic Astrophysics, Austin.
Pauliny-Toth, I. I. K , Wade, C. M., and Heeschen, D. S. 1966, *Ap. J. Suppl.*, No. 116 (in press).
Rowson, B. 1963, *M.N.*, **125**, 177.
Wade, C. M., Clark, B G., and Hogg, D. E 1965, *Ap. J.*, **142**, 406.
Wyndham, J. D. 1966, *A.J.*, **144**, 459.